Supplementary Information

Material and Methods

Selection of target protein and compounds

The 3D crystal structure of the 11β-HSD1 (PDB ID: 1XU9) with best resolution 1.50 Å was obtained in PDB format with co-crystallized molecule CPS [1] and some others 14M, 19V, D3E, and HD2 from PDB IDs: 4HFR, 4HX5, 3D3E, 4BB5,[2–5] and earlier synthesized aminoarylbenzosuberene (AAB) molecules [6] were selected for the study. Discovery studio client (DSC) 2018 was used to prepare the protein structure.[7] The ligand geometry optimization of the AAB and co-crystallized molecules was carried out using energy minimization protocols of Gaussian16 DFT.[8]

Molecular docking study

CDOCKER protocol of DSC 2018 was used for molecular docking of selected molecules with 11β-HSD1 protein.[9] We selected the binding site of co-crystallized molecule CPS as the active site for docking. The binding site coordinates for 11β-HSD1 were X:-10.786; Y:12.998; Z:67.886 with a radius of 10.738 Å. The docking parameters of the CDOCKER protocol were retained default, allowing the production of 10 poses for each selected molecule. The binding energy and two dimensional interactions of the selected molecules with 11β-HSD1 were calculated by running the "Calculate Binding Energy" tab of the CDOCKER. The complexes with the best interaction energy were selected for further MD simulations. Furthermore, we validated the docking protocol by superimposing the co-crystallized 11β-HSD1 and re-docked complex. We saw CPS and NDP bound in a similar way to the binding pocket with a 0.31 Å RMSD value, which demonstrated the robustness of the docking protocol (Figure S10).

Molecular dynamics simulations study

We selected four AAB-11β-HSD1 complexes along with five standard inhibitors for 500 ns of MD simulations conveying GROMOS96 43a1 force field to estimate their stability and validate the docking's correctness.[10–12] For operating the MD Simulations, the ligands topology files were

obtained from the PRODRG server.[13] All established systems were solvated with the single-point charge water model.[14] A cubic box with a volume of 889.61 nm^3 was built for all the selected systems. After executing the gmx genion command, four Na^+ ions were combined, and energy minimization was achieved by applying 50,000 steps of the steepest descent. The simulations were conducted following the cyclic boundary situations with NVT accompanied by an NPT ensemble. Berendsen's coupling and V-rescale algorithms were accepted throughout the restraint MD runs to retain the 300K temperature 1bar pressure constant, respectively.[15,16] The electrostatic linkages were determined by the PME algorithm, with a 12 Å coulomb cutoff.[17] The LINCS algorithm conveyed to constraint the bond lengths.[18] We plotted the Gibbs free energy landscape graphs by using the g_sham script.

Binding free energy study

The binding free energies of all the compounds with Mpro were evaluated to determine complexes stabilization by broadly utilized molecular mechanics Poisson-Boltzmann surface area (MM-PBSA) approach.[19] The g_mmpbsa package engaged in estimating the binding free energies of AAB and experimental inhibitor complexes. Using this approach, evaluation of binding free energy involves computation of Van der Waals, electrostatic, solvent-accessible surface area (SASA), polar, non-polar solvation energies.

Entropy calculation by Quasiharmonic method

The Quasiharmonic (QH) method is proposed by Schlitter to calculate the relative and absolute entropies. These entropies were estimated based on the calculation of the matrix of covariance of Cartesian coordinates using MD simulation. Schlitter’s technique directs only the computation of a determinant, which was the basis for its acceptance in computational biology. In the framework of Schlitter, the absolute entropy approximation illustrates the higher limit of the quantum mechanics entropy.[20]

SMD and umbrella sampling simulations

The ligand unbinds from the protein receptor when a time-dependent external pulling force is applied to a steered MD simulation.[21] Using the GROMACS software 4.6.7, we conducted steered MD simulations.[22] Before beginning the pulling process, we minimized the energy of all the identified protein-ligand structures. We used the external pulling force on the z-axis along the simulated pathway to release the ligand from the receptor protein. The simulation for 500 ns was carried out at the 0.01 nm/ps pull rate and administering a 500 kJ/mol/nm^2 spring constant. We produced the force profiles of every system, selecting the steered MD trajectories. Moreover, we created the distance summary for the production of umbrella sampling slots.[23] Slot spacing of 0.1 nm applied to start center of mass (COM) distance of 3 nm. After that, at each spacing distance of 0.2 nm, we generated sampling windows. A 10 ns simulation run was allotted for every sampling window, finishing in 330 ns of simulation period for each chosen protein-ligand complexes. Then the trajectories were constrained to the WHAM analysis process to produce potential mean force (PMF) graphs. The PMF graph is used to calculate the binding free energies.

Table S1: CDOCKER interaction energy score of selected molecules with 11β-HSD1.

S. No.	Molecules	-CDOCKER Interaction energy
1.	AAB1	42.38
2.	AAB2	44.25
3.	AAB3	44.35
4.	**AAB4**	**48.72**
5.	AAB5	41.54
6.	AAB6	44.38
7.	AAB7	44.59
8.	AAB8	42.88
9.	AAB9	44.28
10.	**AAB10**	**45.99**
11.	AAB11	42.32
12.	**AAB12**	**51.88**
13.	AAB13	40.57
14.	**AAB14**	**47.10**
15.	AAB15	42.63
16.	AAB16	39.77
17.	AAB17	39.21
18.	**CPS**	**76.70**
19.	**14M**	**51.69**
20.	**19V**	**68.65**
21.	**HD2**	**55.75**
22.	**D3E**	**51.83**

* The docked poses were utilized for the calculation of interaction energies of the co-crystallized molecules.

Table S2. Binding free energy calculations of selected 11β-HSD1 complexes using MM-PBSA.

11β-HSD1 Complexes with	ΔE binding (kJ/mol)	ΔE Van der Waal (kJ/mol)	SASA (kJ/mol)	ΔE Electrostatic (kJ/mol)	ΔE polar solvation (kJ/mol)
CPS	-118.627	-228.213	-22.893	-73.865	206.343
D3E	-61.822	-187.081	-19.851	-279.713	424.823
14M	-185.436	-160.949	-16.703	-235.245	227.461
19V	-150.831	-252.841	-23.273	-120.256	245.539
HD2	-96.619	-130.997	-14.255	-23.346	71.979
AAB4	-221.551	-231.492	-19.775	-3.023	32.739
AAB10	-148.241	-275.043	-20.965	-25.521	173.288
AAB12	-131.051	-206.472	-19.307	-4.05	98.780
AAB14	-138.355	-269.495	-22.369	-10.257	163.766

Table S3. Quantum-mechanical quasi-harmonic configurational entropy values for the selected complexes.

S. No.	Complexes	Entropy (J/mol K)
1.	11β-HSD1-apo	34112.1
2.	11β-HSD1-CPS	33629.1
3.	11β-HSD1-D3E	32888.9
4.	11β-HSD1-14M	34541.6
5.	11β-HSD1-19V	32409.5
6.	11β-HSD1-HD2	34190.5
7.	11β-HSD1-AAB4	32704.6
8.	11β-HSD1-AAB10	32729.3
9.	11β-HSD1-AAB12	31640.8
10.	11β-HSD1-AAB14	32602.5

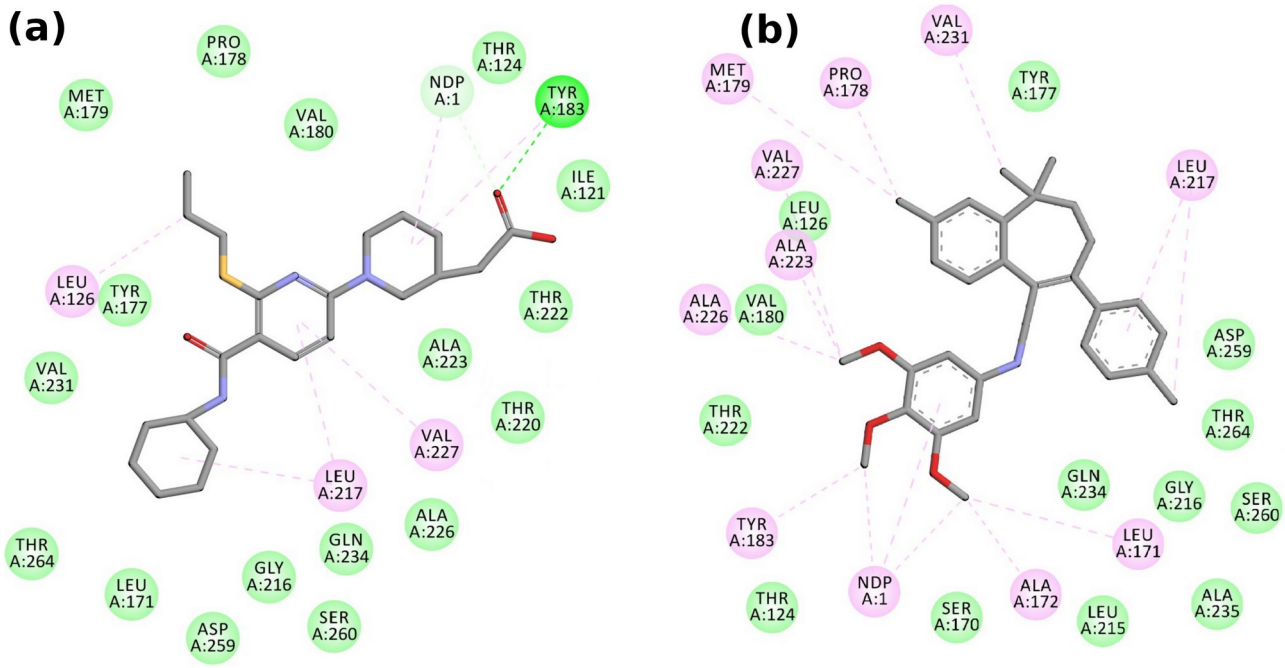

Figure S1. 2-D interactions of 11β-HSD1 with the selected molecules (a) 14M, (b) AAB4.

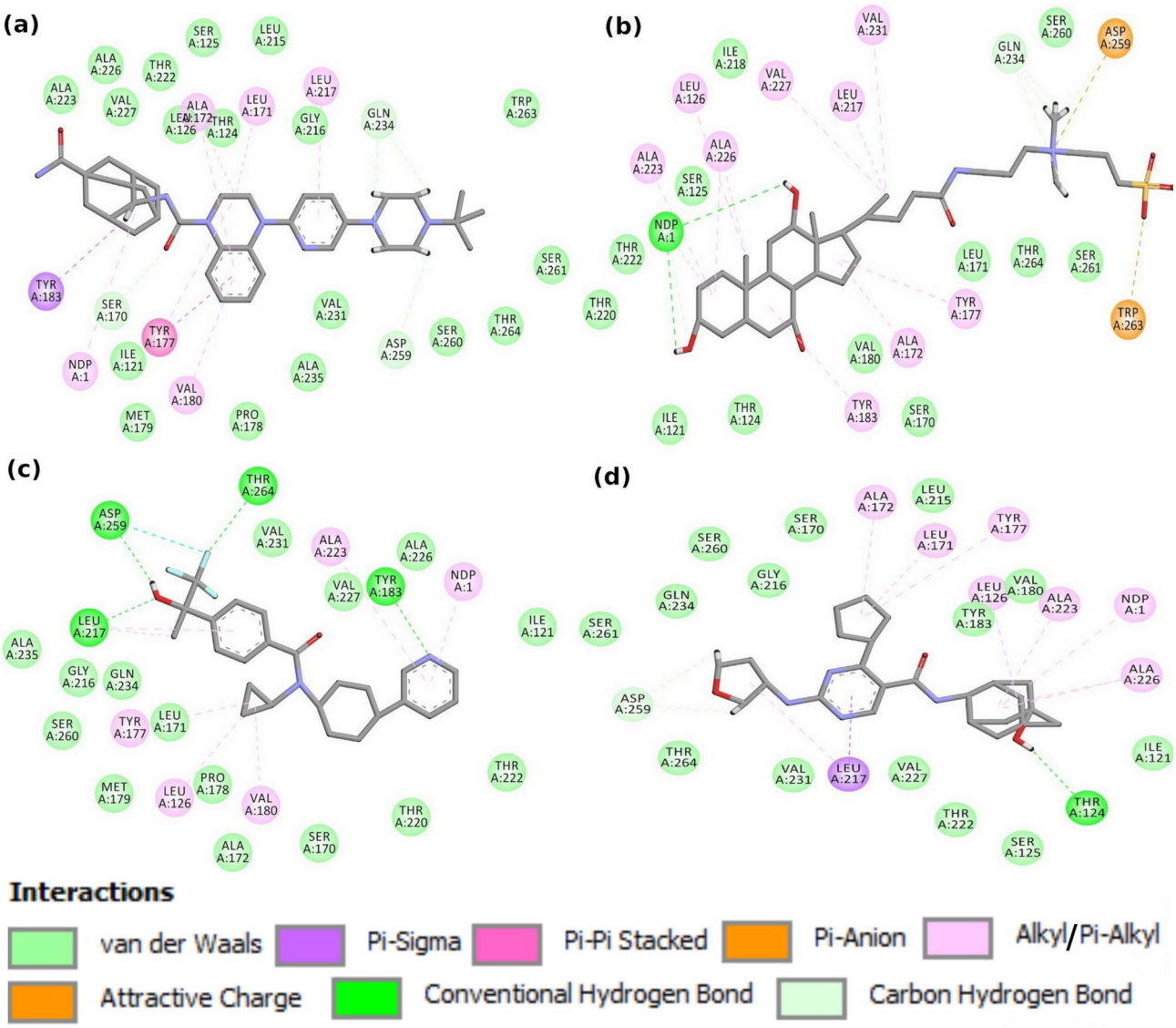

Figure S2. 2D interactions of 11β-HSD1 with standard molecules (a) 19V, (b) CPS, (c) D3E, and (d) HD2.

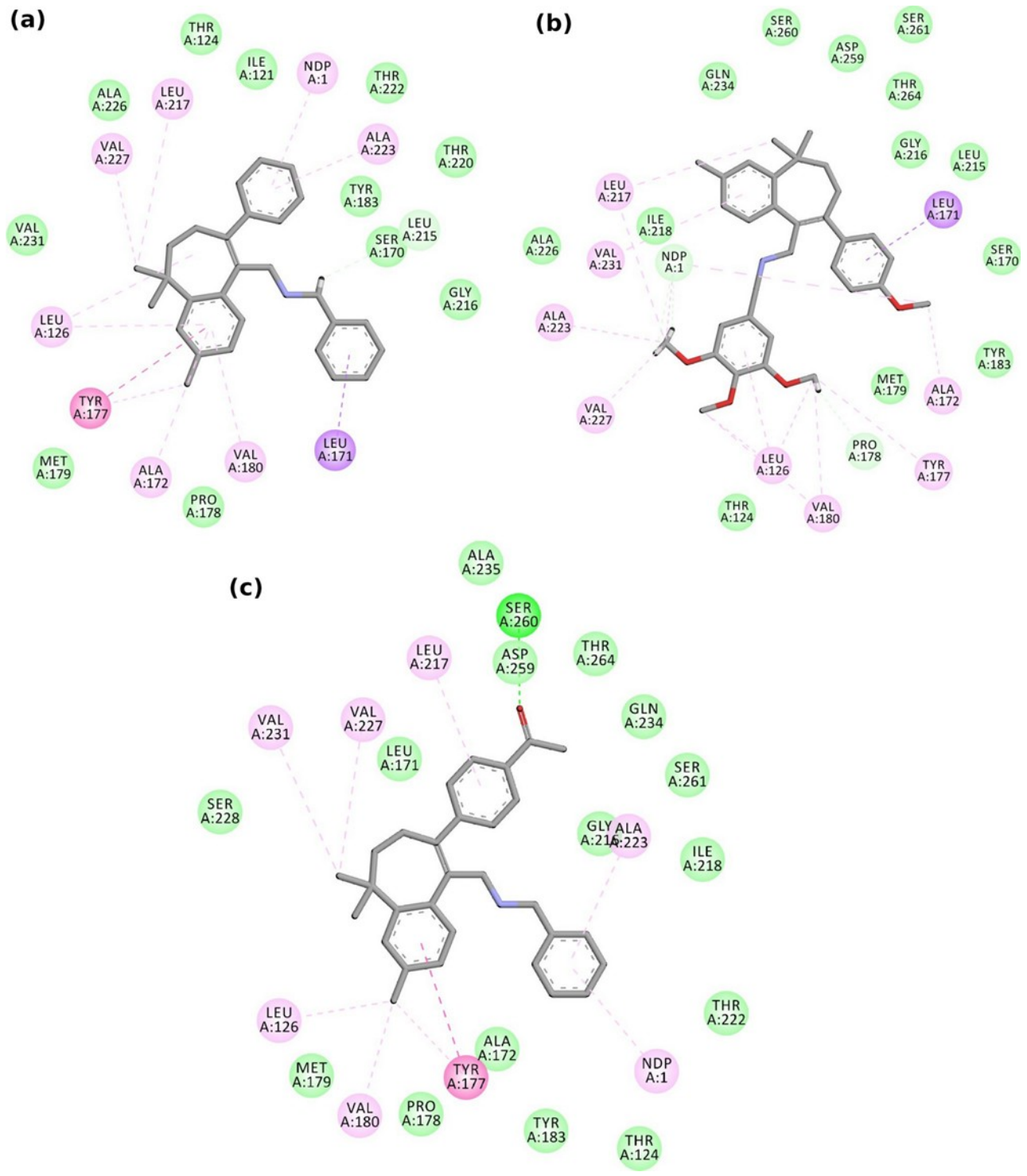

Figure S3. 2D interactions of 11β-HSD1 with AAB molecules (a) AAB10, (b) AAB12, and (c) AAB14.

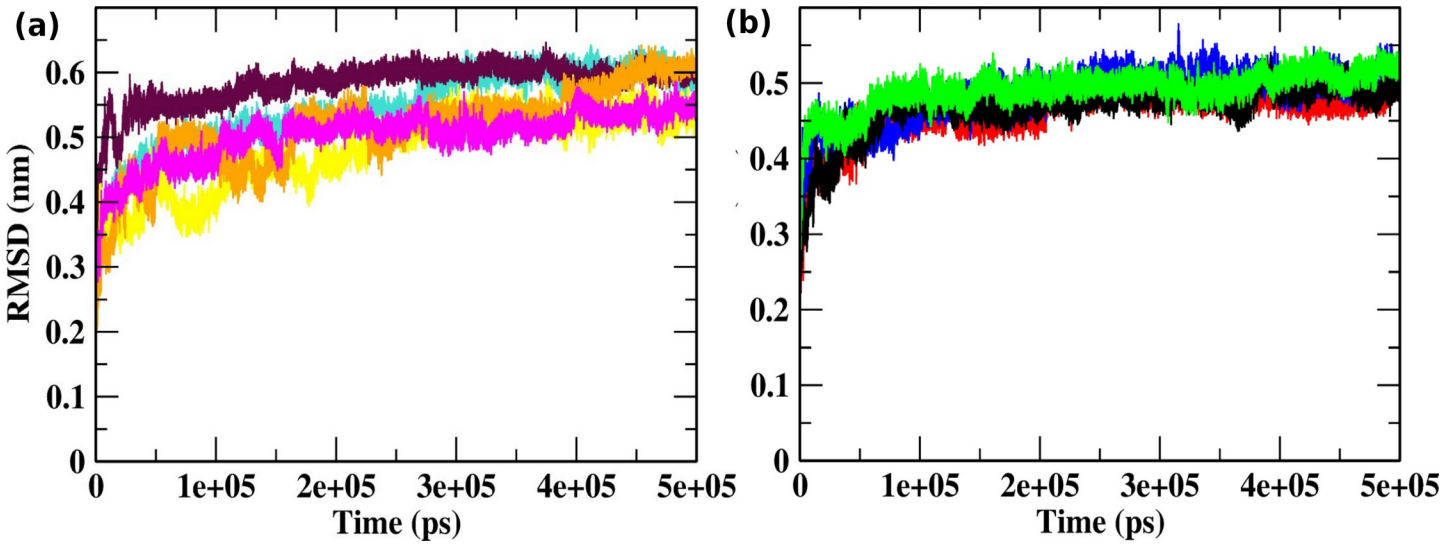

Figure S4. Backbone RMSDs are shown as a function of time for the 11β-HSD1 complexes with co-crystallized molecules **(a)** CPS (cyan), 14M (magenta), 19V (orange), HD2 (yellow), D3E (maroon). **(b)** AAB4 (black), AAB12 (red), AAB14 (green), AAB10 (blue).

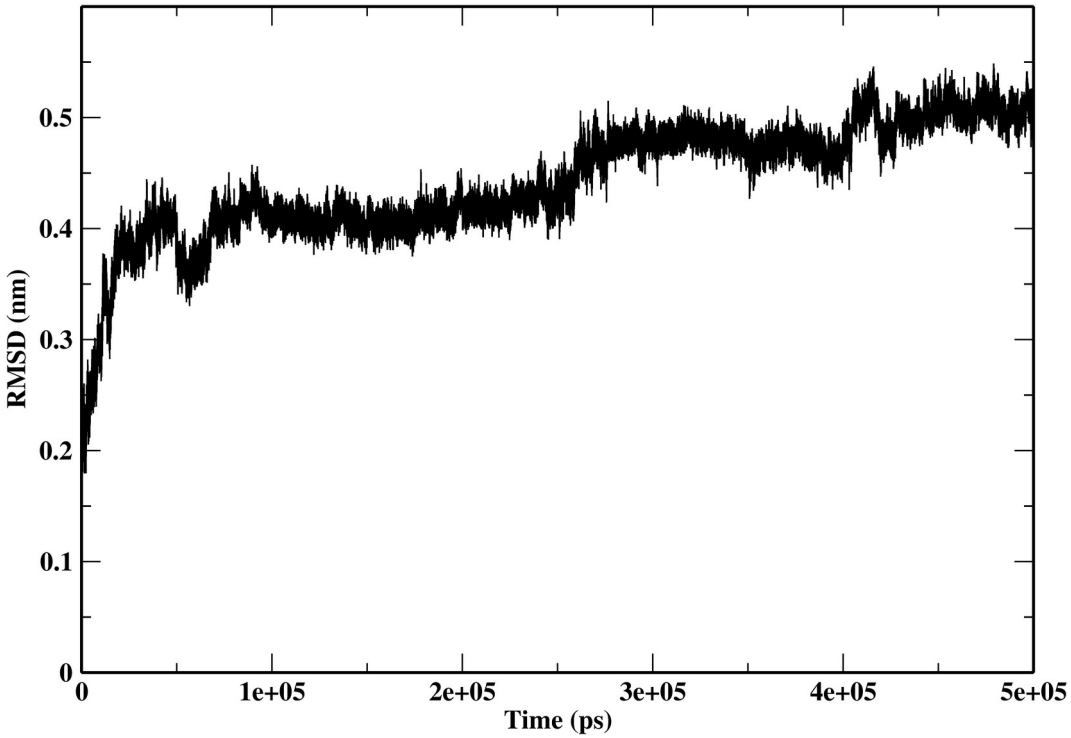

Figure S5. Backbone RMSD shown as a function of time for the Apo-11β-HSD1 protein.

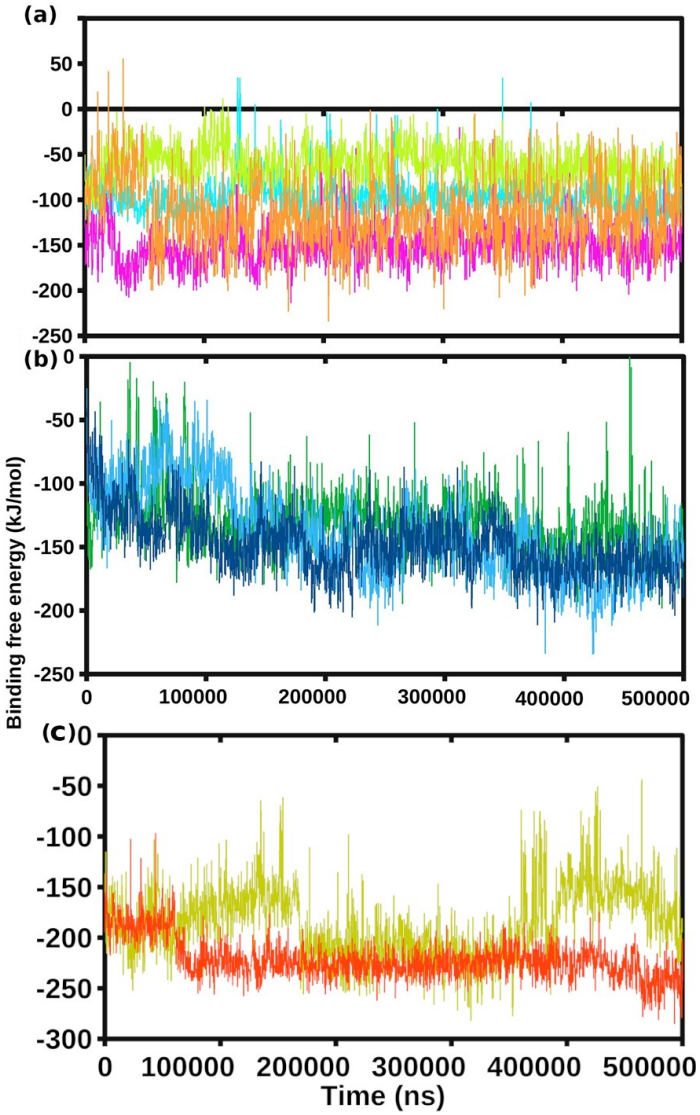

Figure S6. Graphical representation of binding free energy of 11β-HSD1 in complex with (a) CPS (orange), 19V (magenta), HD2 (cyan), D3E (light green). (b) AAB10 (blue), AAB12 (dark green), AAB14 (sky blue). (c) 14M (olive) and AAB4 (dark orange).

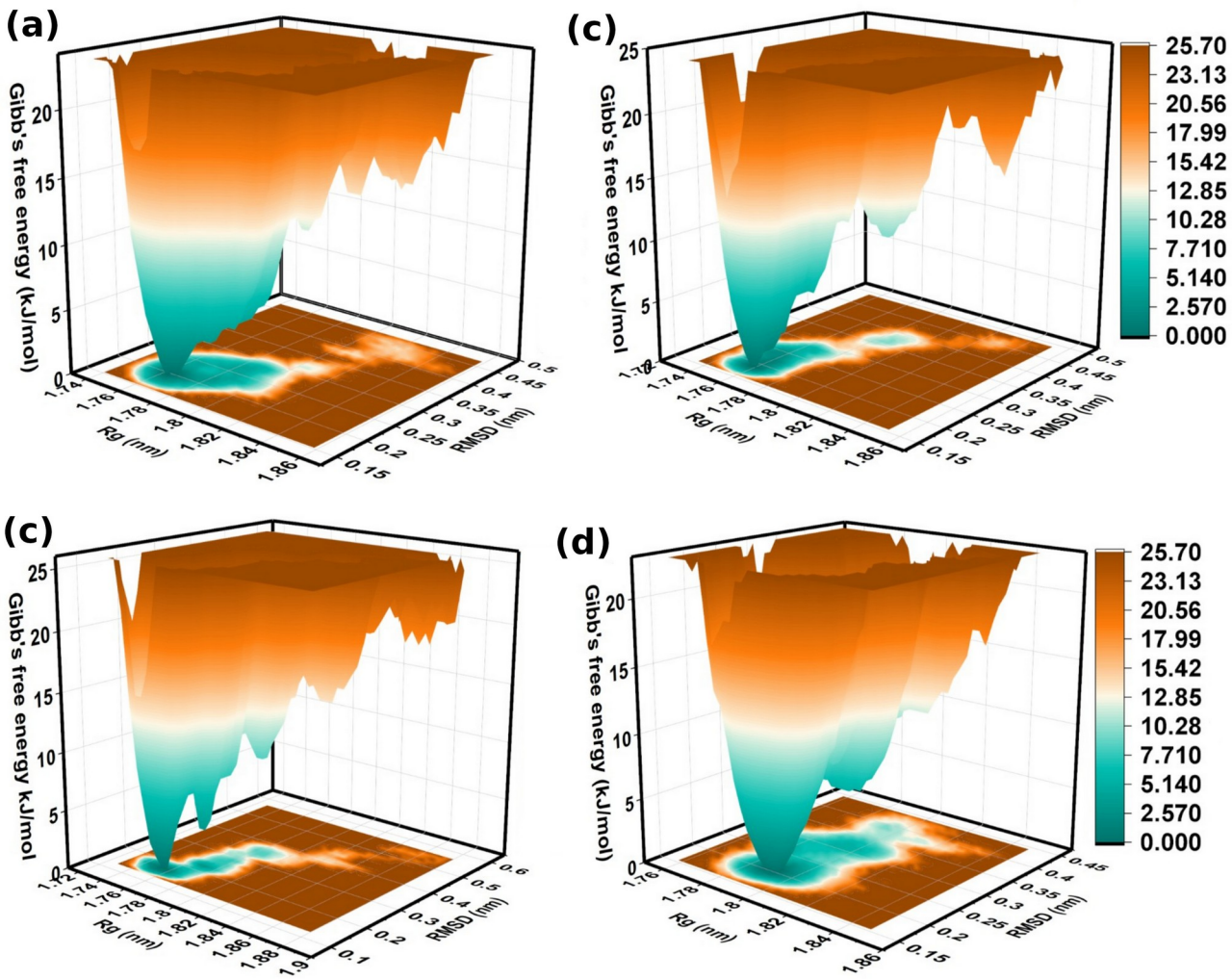

Figure S7. The 2D and 3D free energy landscapes from MD trajectories for four 11β-HSD1 complexes (a) CPS, (b) 19V, (c) HD2 (d) D3E. The dark ocean green color region shows the minimum energy conformation.

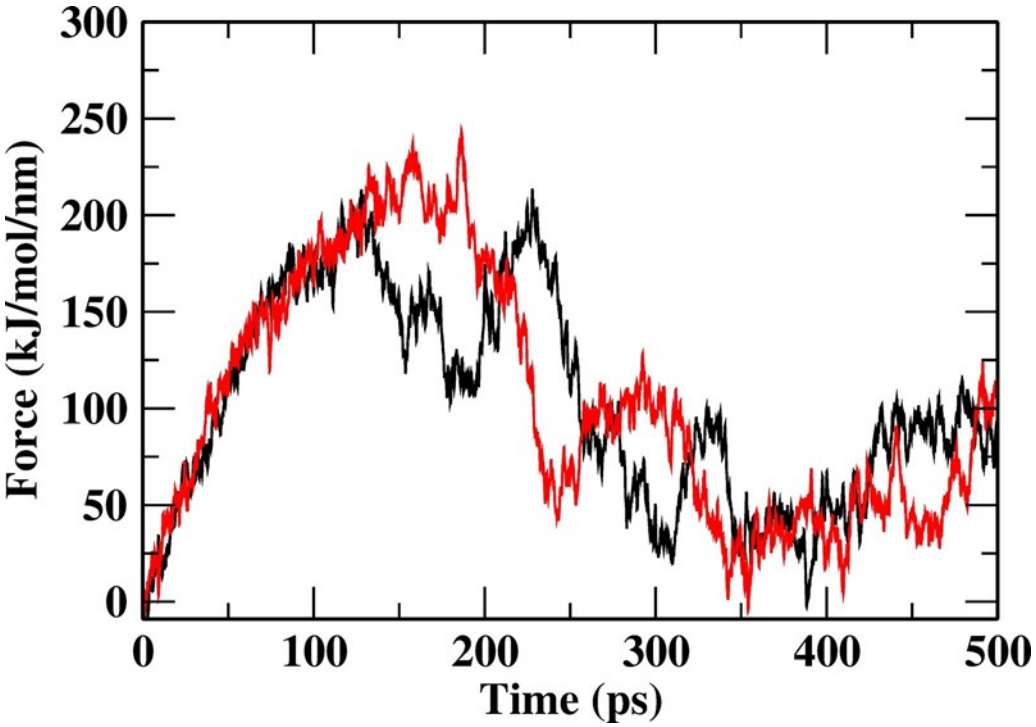

Figure S8. The external pulling force applied to unbind 14M (black) and AAB4 (red) from 11β-HSD1 protein during SMD simulations.

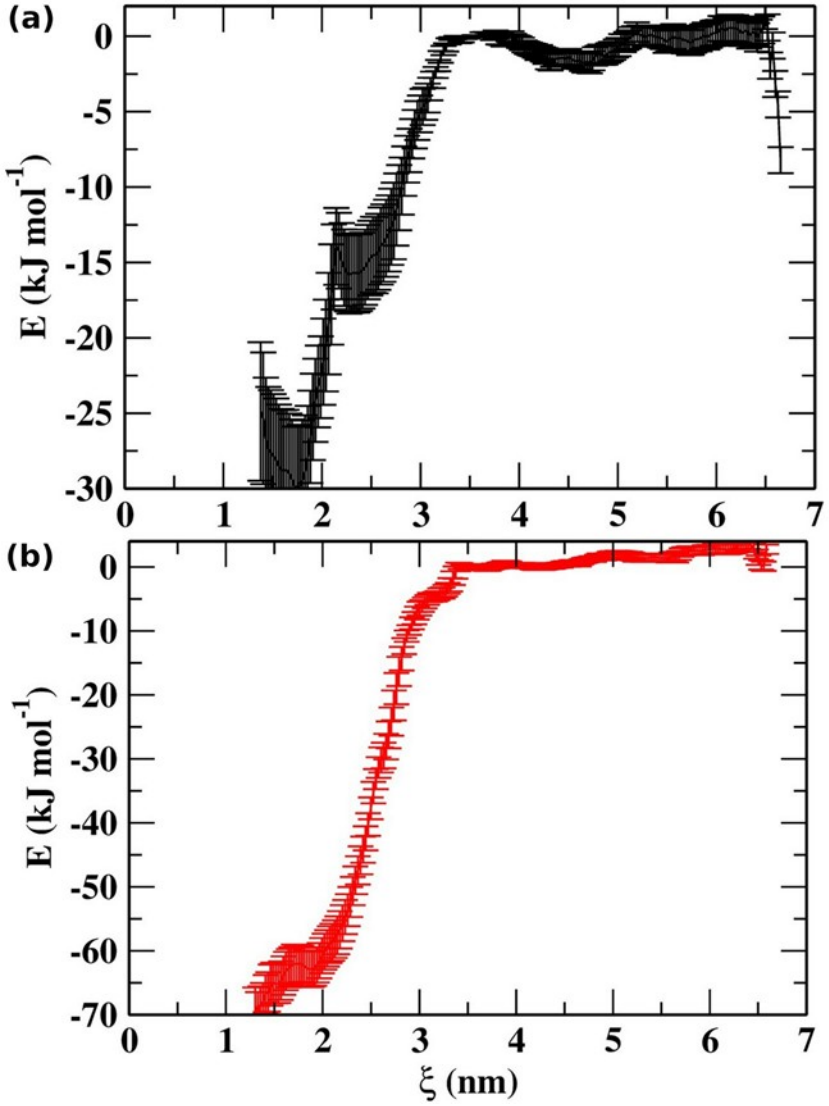

Figure S9. The external pulling force error bars estimated by the bootstrap methods showing unbinding of 14M (black) and AAB4 (red) from 11β-HSD1 protein during SMD simulations.

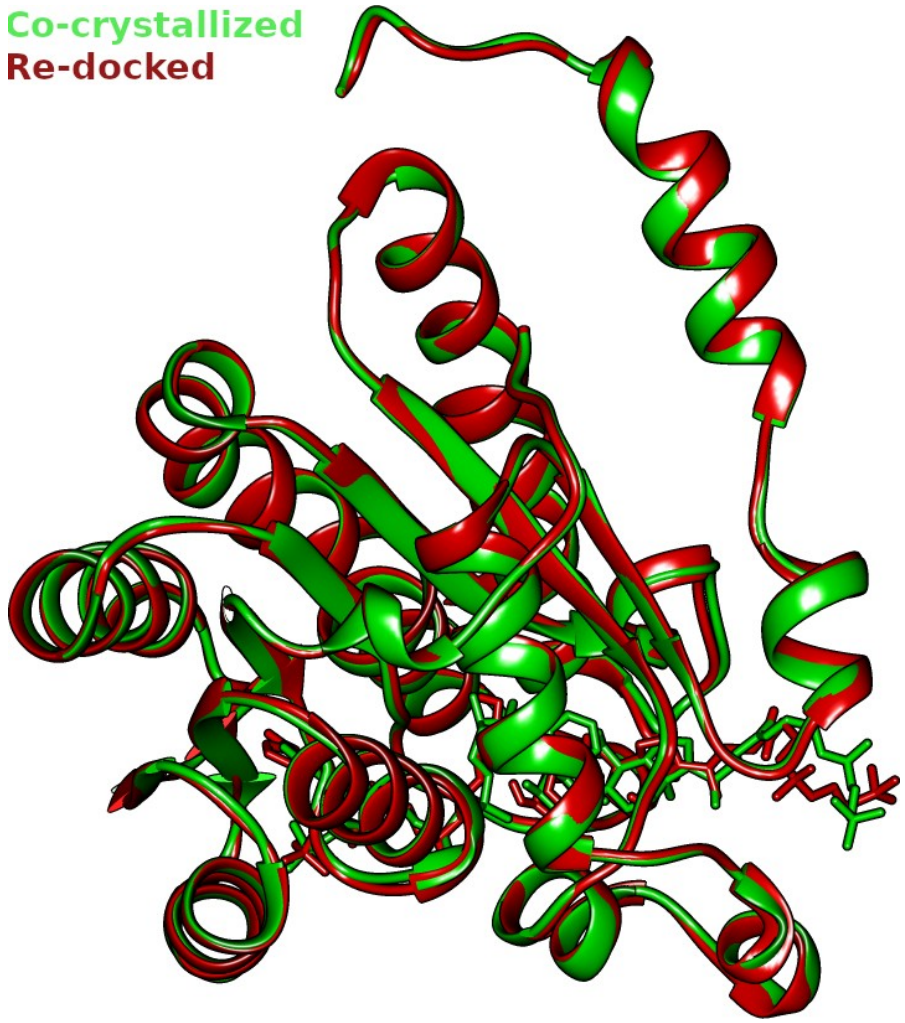

Figure S10: Superimposed protein three dimensional X-ray co-crystal structure of 11β-HSD1 (green) and re-docked (maroon).

References:

1. Hosfield DJ, Wu Y, Skene EJ, et al. Conformational flexibility in crystal structures of human 11β-hydroxysteroid dehydrogenase type I provide insights into glucocorticoid interconversion and enzyme regulation. *J Biol Chem*. 2005;280(6):4639-4648. doi:10.1074/jbc.M411104200

2. Scott JS, Bowker SS, Deschoolmeester J, et al. Discovery of a potent, selective, and orally bioavailable acidic 11β-hydroxysteroid dehydrogenase type 1 (11β-HSD1) inhibitor: Discovery of 2-[(3 s)-1-[5-(cyclohexylcarbamoyl)-6-propylsulfanylpyridin-2-yl]- 3-piperidyl]acetic acid (AZD4017). *J Med Chem*. 2012;55(12):5951-5964. doi:10.1021/jm300592r

3. Venier O, Pascal C, Braun A, et al. Discovery of SAR184841, a potent and long-lasting inhibitor of 11β-hydroxysteroid dehydrogenase type 1, active in a physiopathological animal model of T2D. *Bioorganic Med Chem Lett*. 2013;23(8):2414-2421. doi:10.1016/j.bmcl.2013.02.018

4. Julian LD, Wang Z, Bostick T, et al. Discovery of novel, potent benzamide inhibitors of 11β-hydroxysteroid dehydrogenase type 1 (11β-HSD1) exhibiting oral activity in an enzyme inhibition ex vivo model. *J Med Chem*. 2008;51(13):3953-3960. doi:10.1021/jm800310g

5. Goldberg FW, Leach AG, Scott JS, et al. Free-wilson and structural approaches to Co-optimizing human and rodent isoform potency for 11β-hydroxysteroid dehydrogenase type 1 (11β-HSD1) inhibitors. *J Med Chem*. 2012;55(23):10652-10661. doi:10.1021/jm3013163

6. Bharti R, Bal Reddy C, Kumar S, Das P. Supported palladium nanoparticle-catalysed Suzuki–Miyaura cross-coupling approach for synthesis of aminoarylbenzosuberene analogues from natural precursor. *Appl Organomet Chem*. 2017;31(11). doi:10.1002/aoc.3749

7. Studio D. Dassault Systemes BIOVIA, Discovery Studio Modelling Environment, Release 4.5. *Accelrys Softw Inc*. Published online 2015:98-104.

8. Zheng J, Frisch MJ. Efficient Geometry Minimization and Transition Structure Optimization Using Interpolated Potential Energy Surfaces and Iteratively Updated Hessians. *J Chem Theory Comput*. 2017;13(12):6424-6432. doi:10.1021/acs.jctc.7b00719

9. Brooks BR, Bruccoleri RE, Olafson BD, States DJ, Swaminathan S, Karplus M. CHARMM: A program for macromolecular energy, minimization, and dynamics calculations. *J Comput Chem*. 1983;4(2):187-217. doi:10.1002/jcc.540040211

10. M.J A, D. van de Rs, E L, B H, GROMACS Development Team. GROMACS User Manual version 5.0.5. *www.gromacs.org*. Published online 2015. http://www.gromacs.org/

11. Hess B, Kutzner C, Van Der Spoel D, Lindahl E. GRGMACS 4: Algorithms for highly efficient, load-balanced, and scalable molecular simulation. *J Chem Theory Comput*. 2008;4(3):435-447. doi:10.1021/ct700301q

12. Van Der Spoel D, Lindahl E, Hess B, Groenhof G, Mark AE, Berendsen HJC. GROMACS: Fast, flexible, and free. *J Comput Chem*. 2005;26(16):1701-1718. doi:10.1002/jcc.20291

13. Schüttelkopf AW, Van Aalten DMF. PRODRG: A tool for high-throughput crystallography of protein-ligand complexes. *Acta Crystallogr Sect D Biol Crystallogr*. 2004;60(8):1355-1363. doi:10.1107/S0907444904011679

14. Berendsen HJC, Grigera JR, Straatsma TP. The missing term in effective pair potentials. *J Phys Chem*. 1987;91(24):6269-6271. doi:10.1021/j100308a038

15. Berendsen HJC, Postma JPM, Van Gunsteren WF, Dinola A, Haak JR. Molecular dynamics with coupling to an external bath. *J Chem Phys*. 1984;81(8):3684-3690. doi:10.1063/1.448118

16. Parrinello M, Rahman A. Polymorphic transitions in single crystals: A new molecular dynamics method. *J Appl Phys*. 1981;52(12):7182-7190. doi:10.1063/1.328693

17. Darden T, York D, Pedersen L. Particle mesh Ewald: An N·log(N) method for Ewald sums in large systems. *J Chem Phys*. 1993;98(12):10089-10092. doi:10.1063/1.464397

18. Hess B, Bekker H, Berendsen HJC, Fraaije JGEM. LINCS: A Linear Constraint Solver for molecular simulations. *J Comput Chem*. 1997;18(12):1463-1472. doi:10.1002/(SICI)1096-987X(199709)18:12<1463::AID-JCC4>3.0.CO;2-H

19. Kumari R, Kumar R, Lynn A. G-mmpbsa -A GROMACS tool for high-throughput MM-PBSA calculations. *J Chem Inf Model*. 2014;54(7):1951-1962. doi:10.1021/ci500020m

20. Schlitter J. Estimation of absolute and relative entropies of macromolecules using the covariance matrix. *Chem Phys Lett*. 1993;215(6):617-621. doi:10.1016/0009-2614(93)89366-P

21. Izrailev S, Stepaniants S, Isralewitz B, et al. Steered Molecular Dynamics. Published online 1999:39-65. doi:10.1007/978-3-642-58360-5_2

22. Do PC, Lee EH, Le L. Steered Molecular Dynamics Simulation in Rational Drug Design. *J Chem Inf Model*. 2018;58(8):1473-1482. doi:10.1021/acs.jcim.8b00261

23. Hub JS, De Groot BL, Van Der Spoel D. G-whams-a free Weighted Histogram Analysis implementation including robust error and autocorrelation estimates. *J Chem Theory Comput*. 2010;6(12):3713-3720. doi:10.1021/ct100494z